

Supplemental Data

Analysis of U8 snoRNA Variants in Zebrafish Reveals How Bi-allelic Variants Cause Leukoencephalopathy with Calcifications and Cysts

Andrew P. Badrock, Carolina Uggenti, Ludivine Wacheul, Siobhan Crilly, Emma M. Jenkinson, Gillian I. Rice, Paul R. Kasher, Denis L.J. Lafontaine, Yanick J. Crow, and Raymond T. O'Keefe

28S binding

SNORD11B	AT <ins>CGTCAGGTGGATAATCCTTACCTGTTCCCTCCGGAGGGCAGA</ins> —T
U8-1	G— <ins>CATCAGTGAGGTTATCCTTACCTGTTG</ins> —TCTT—A—GA AATAAGACTA
U8-2	A— <ins>CATCAGTGAGGTTGTCC</ins> —TACCTGTT—T—A—GAAATAAGACTT
U8-3	A— <ins>CATCAGTGAGGTAATCCTTACCTGTTA</ins> —CCTT—A—GCAATAAGGTAA
U8-4	G T— <ins>ATCAGTGAGGTTATCCTTACCTGTTG</ins> —TCTT—A—GAAATAAGACTG
U8-5	G— <ins>CATCAGTGAGGTTATCCTTGCCTGTTG</ins> —TCTT—A—GA ATTAAGACTT

* * * * * * * * * * * *

C box	LSm binding motif
SNORD11B	TAGAAC <ins>ATGATGATTGGAGATGCATGAA</ins> —A <ins>CGTGATTAACGT</ins> —CTCT
U8-1	CAGCAC <ins>ATGATGATTGGAT</ins> —TCTATGAAATG <ins>CGTGATTA</ins> TATT—CTGT
U8-2	CAGCAC <ins>ATGATGATTGGAT</ins> —TCTATGAAATAT <ins>GTGATTA</ins> TATT—CTGT
U8-3	CAGATC <ins>ATGATGATTGGAT</ins> —TCTATGAAATAC <ins>CGTGATTA</ins> TGTT—CCGT
U8-4	CAGTAT <ins>ATGATGATTGGAT</ins> —TCTATGAAATAT <ins>GTGACTATGTTGTACTGT</ins>
U8-5	CAGCAC <ins>ATGATGATTGGAT</ins> —TCTATGAAATAC <ins>ATGATTA</ins> TACT—CTGT

* * * * * * * * * * * *

D box	
SNORD11B	GCGTAATCAGGACTTGCAACACCCCTGATTGCTCCGT <ins>CTGATT</ins>
U8-1	ATTCTTAAAGGGTTTGCAACACCTTATGAAATCCTGT <ins>CTGA</ins> —T
U8-2	ATT CGTATAGGGTT CACA ACT—CTGGATCCTATGT <ins>CTGA</ins> —T
U8-3	ATTTGT TAGGGACTGCAACCCCTTACGAAATCCTGT <ins>CTGA</ins> —C
U8-4	ATTTGTACATGACTTGCAACCTCTTATAAAATCCTAT <ins>CTGA</ins> —T
U8-5	GTTCATA TAGGGCTTGTACCCATTATGAAATCCTGT <ins>CTGA</ins> —T

* * * * * * * * * * * *

Figure S1. Human U8 and zebrafish U8 1-5 mature sequences exhibit extensive conservation

Mature human U8 and zebrafish U8 1-5 sequences were aligned using ClustalW (<https://www.ebi.ac.uk/Tools/msa/tcoffee/>). * denotes conserved nucleotides.

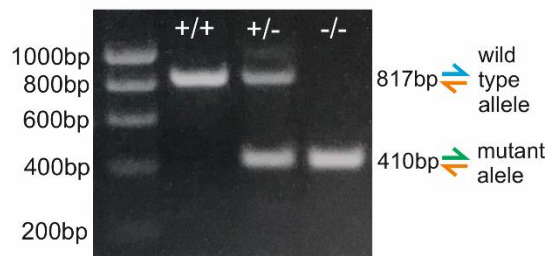
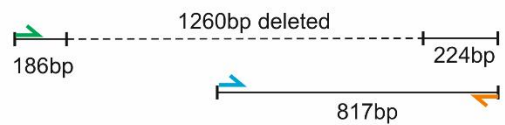
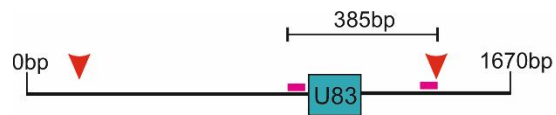


Figure S2. The Δ U8-3 mutant is homozygous for a 1.26kb deletion encompassing the *U8-3* gene locus

Schematic depicting the genotyping strategy for the zebrafish Δ U8-3 mutant. Two sgRNAs predicted to excise 385bp encompassing the *U8-3* gene are represented by pink bars. Red arrowheads depict actual excision sites that delete 1260bp (dashed line) encompassing the *U8-3* gene locus. A three primer PCR was performed to genotype whereby 817bp (blue, orange primer) is amplified in the presence of a wildtype copy of *U8-3* and 410bp (green, orange primer) amplified in the presence of a deleted Δ U8-3 allele. bp, base pairs.

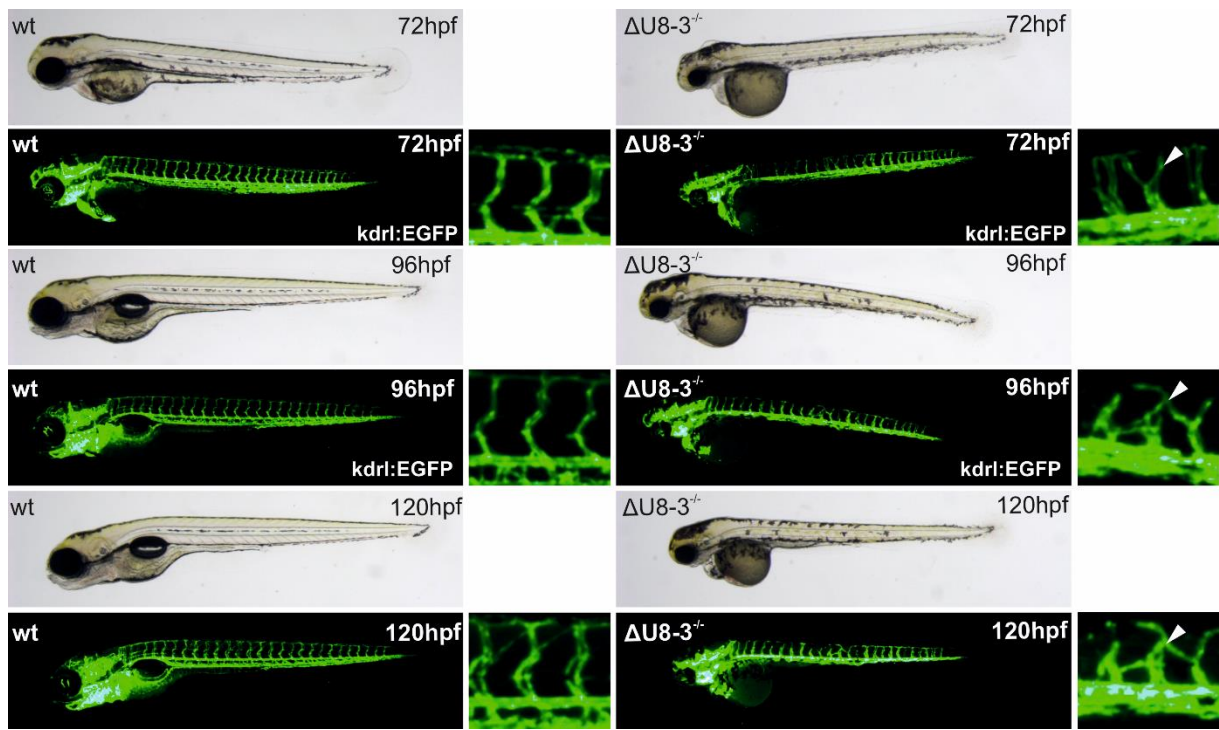


Figure S3. The $\Delta U8-3$ mutant exhibits a range of gross morphological abnormalities and comes to a developmental standstill

From 72hpf $\Delta U8-3$ mutants display impaired yolk resorption, reduced craniofacial structures and hindbrain swelling. By 96hpf $\Delta U8-3$ mutants fail to inflate their swim bladders, display an underdeveloped intestine, and by 120hpf display cardiac oedema. At all stages disorganized trunk vasculature is observed (white arrowheads) when compared to wildtype (inserts).

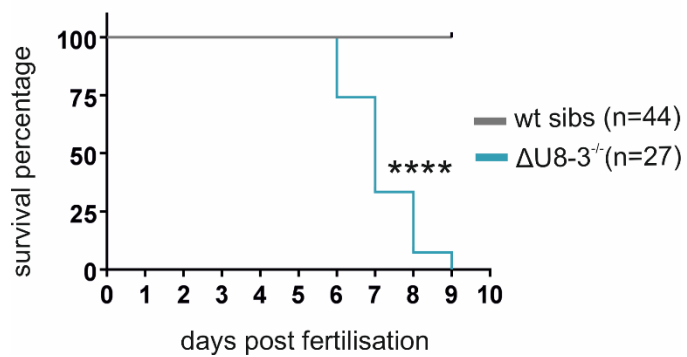


Figure S4. The $\Delta U8-3$ mutant phenotype is lethal

Kaplain-Meier plot demonstrating that $\Delta U8-3$ mutants begin to die from 6dpf and exhibit 100% mortality by 9dpf. dpf - days post fertilization.

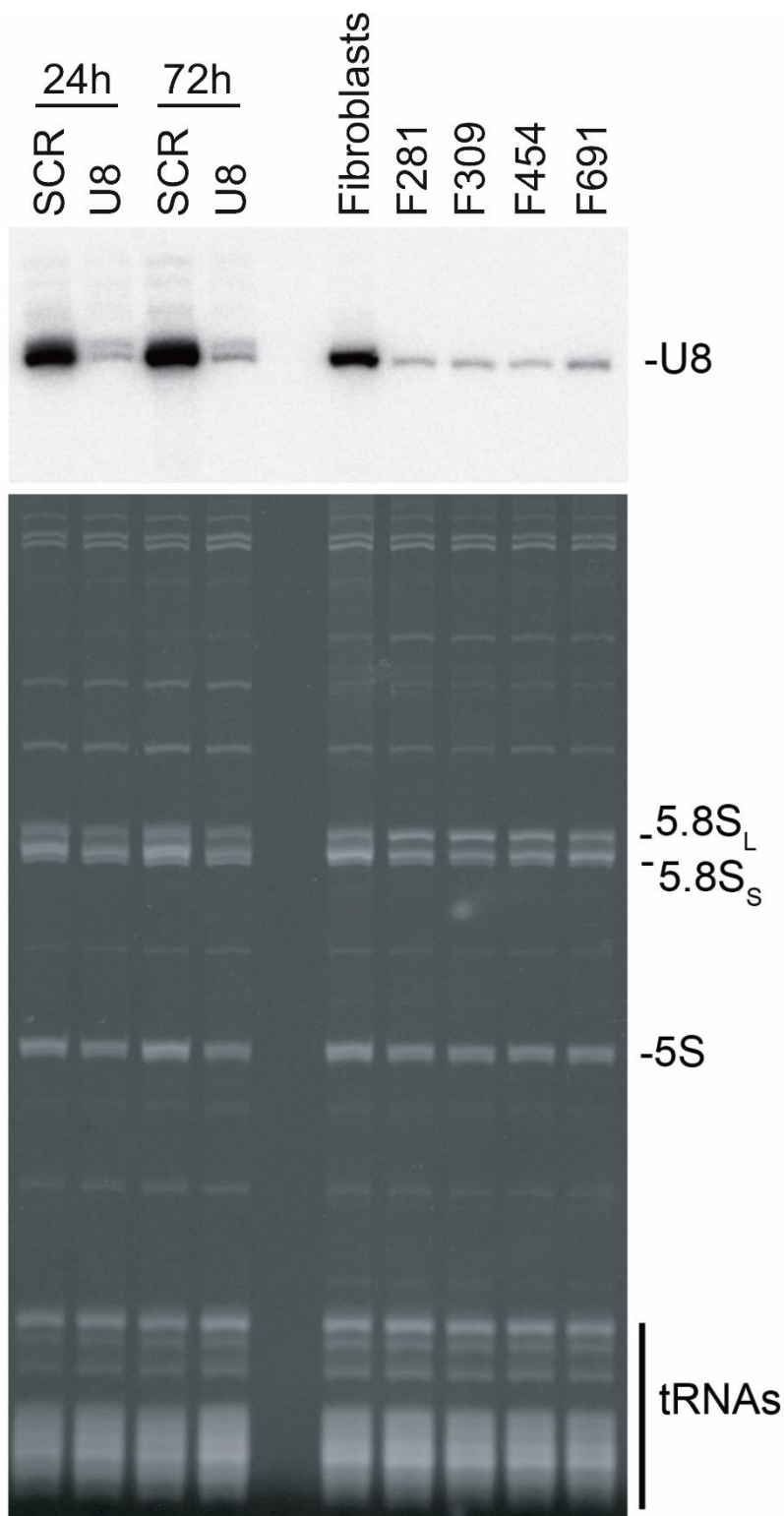


Figure S5. LCC fibroblasts express less total U8 compared to wildtype fibroblasts

Northern blot analysis with a probe specific to U8 snoRNA. U8 expression is shown after ASO-mediated depletion of human U8 snoRNA from HCT116 cells in which rRNA processing was analyzed (see Figure 2E), or in LCC fibroblast cell lines F281, F309, F454 and F691. ASO – antisense oligonucleotide. The same amount of total RNA (OD_{260}) was loaded in each lane of the gel. Ethidium bromide staining of the acrylamide gel demonstrates equal loading, as determined by tRNAs which are produced independently.

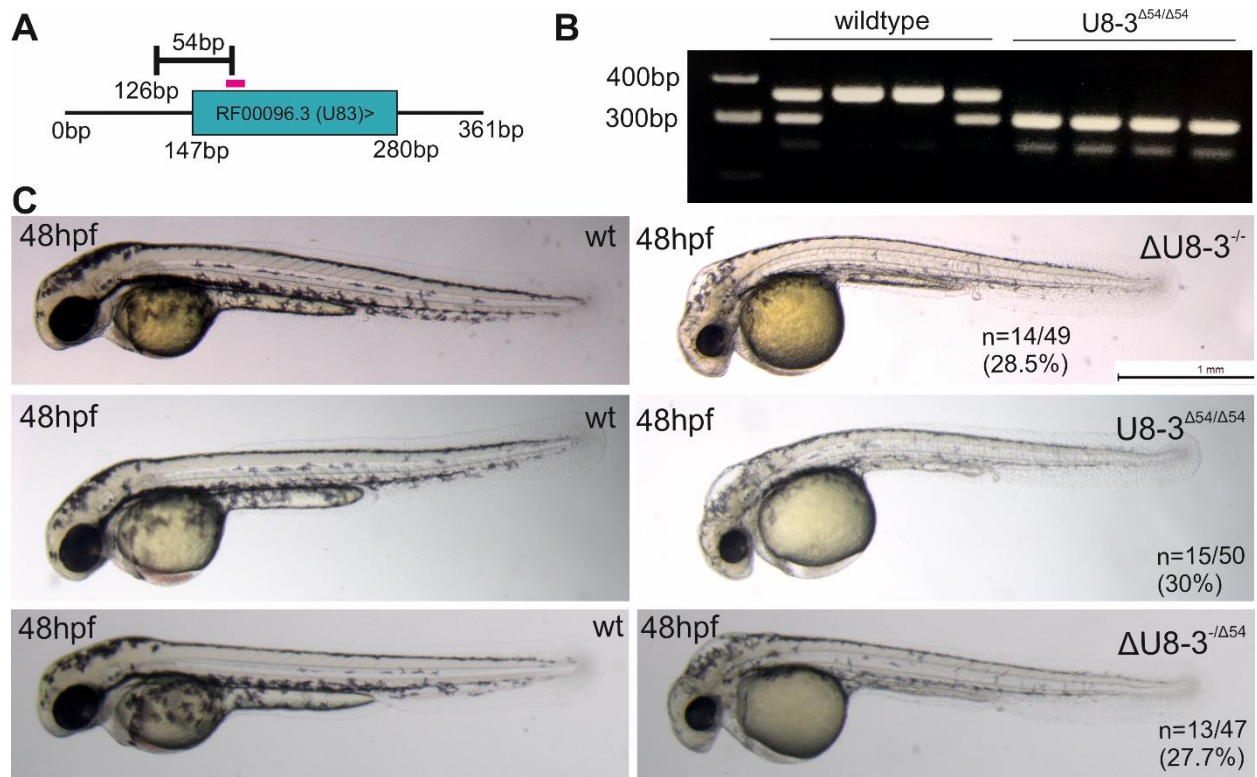


Figure S6. Non-complementation with independent mutant alleles of *U8-3* demonstrates that the $\Delta\text{U8-3}$ mutant phenotype is specific

A) Schematic depicting the 54bp deletion allele ($\Delta\text{54U8-3}$) generated with an independent sgRNA (pink bar) from the sgRNAs used to excise *U8-3* shown in Figure 2A.

B) Genotyping demonstrates the 54bp deletion (307bp band) segregates with the *U8-3* mutant phenotype.

C) Both $\Delta\text{U8-3}$ and $\Delta\text{54U8-3}$ alleles display mendelian recessive inheritance i.e. approximately 25% of mutant progeny are produced from incrossing heterozygous carriers. When heterozygous carriers of each allele were crossed to each other non-complementation (failure to produce 100% wildtype progeny) was observed, demonstrating the alleles result from loss-of-function in the same gene.

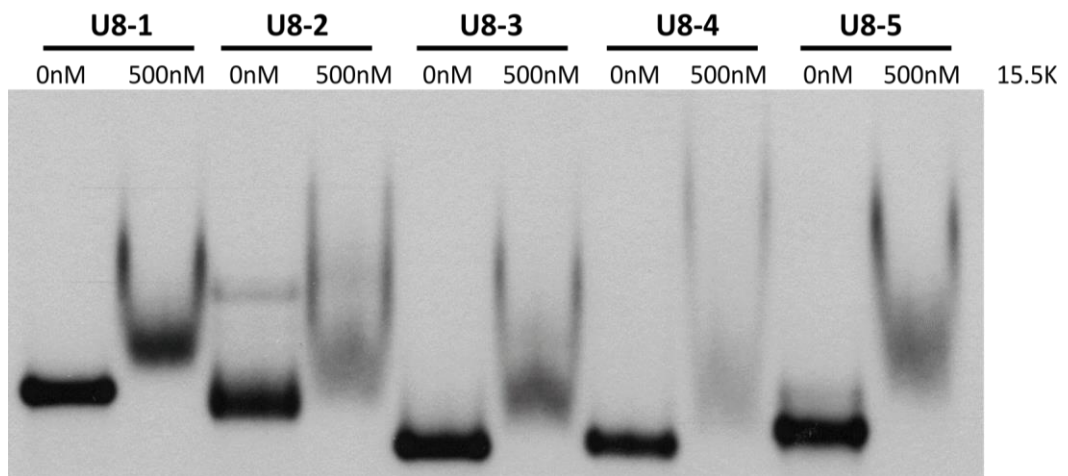


Figure S7. EMSAs demonstrates all five zebrafish U8s bind 15.5K

Protein binding of zebrafish U8 variants. Electrophoretic mobility shift assays (EMSA) using 5'-end-radiolabeled *in vitro* transcribed mature zebrafish *U8-1*, *U8-2*, *U8-3*, *U8-4* and *U8-5* with 500nM of His₆-tagged 15.5K human protein (15.5K). Binding of 15.5K to zebrafish U8 is indicated by a mobility shift.

3' processed region
3' BOX

 human U8 CTTTCTGACGATCACTTACATTGT GTTATGCTGATTAGCAGA
 zebrafish U8-3 ACAT TTT AATAACC GTTT CAAAATCGA

Figure S8. Alignment of human U8 and zebrafish U8-3 3' extension sequences

Human and putative zebrafish 3' extension sequences (blue) are divergent. A 3' BOX is predicted for zebrafish U8-3 (pink) according to the 3' BOX consensus sequence (black).

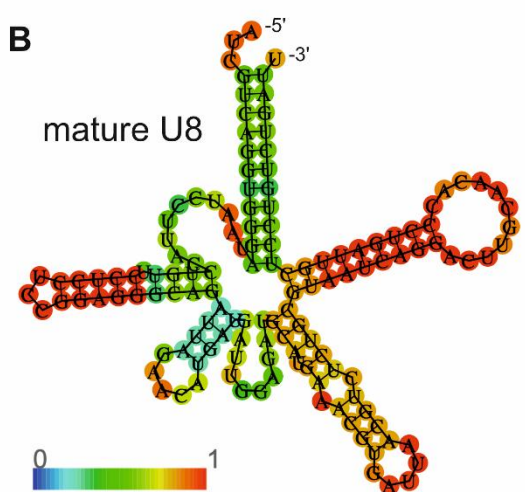
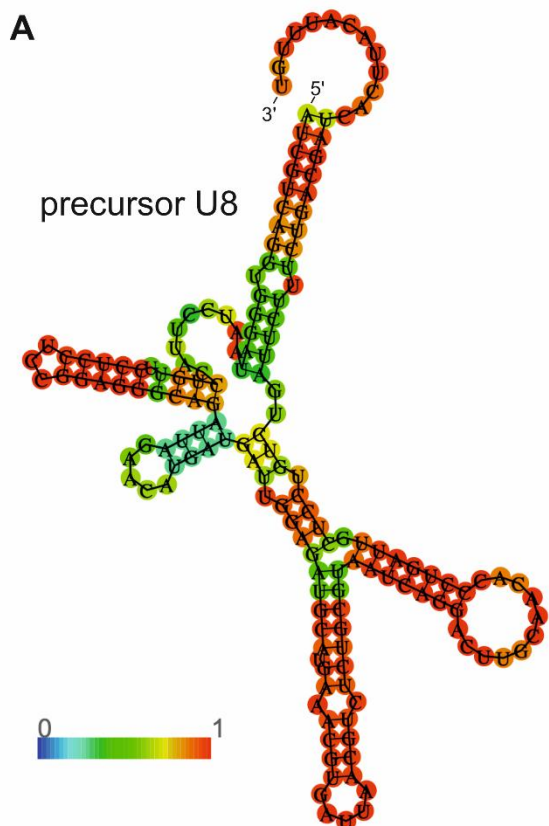


Figure S9. Minimum free energy secondary structure predictions of precursor and mature human U8

A) Minimum free energy secondary structure prediction by RNA fold of the precursor human U8. Duplex formation between the 5' end and 3' extension is predicted with high probability. The probability of each base-pairing interaction is represented by a colormetric scale ranging from 0 (blue) to 1 (red).

B) Minimum free energy secondary structure prediction by RNA fold of the mature human U8. Duplex formation between the 5' end and 3' end is predicted with low probability. The probability of each base-pairing interaction is represented by a colormetric scale ranging from 0 (blue) to 1 (red).

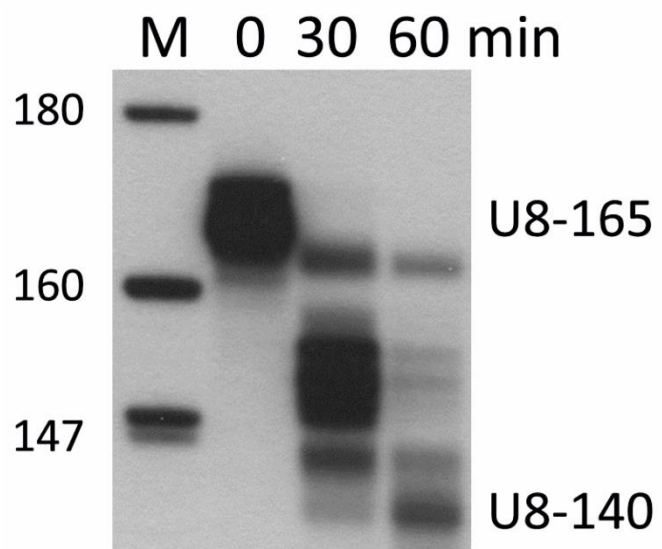


Figure S10. Time course of wild type human pre-U8 snoRNA processing.

Processing of 5' end-radiolabelled *in vitro* transcribed precursor U8 wildtype snoRNA (U8-165) was assessed in HeLa nuclear extracts at 0, 30 and 60 minutes (min) to monitor production of mature U8 (U8-140). Mature U8 is clearly present after 60 min of processing.

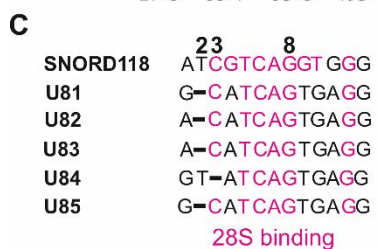
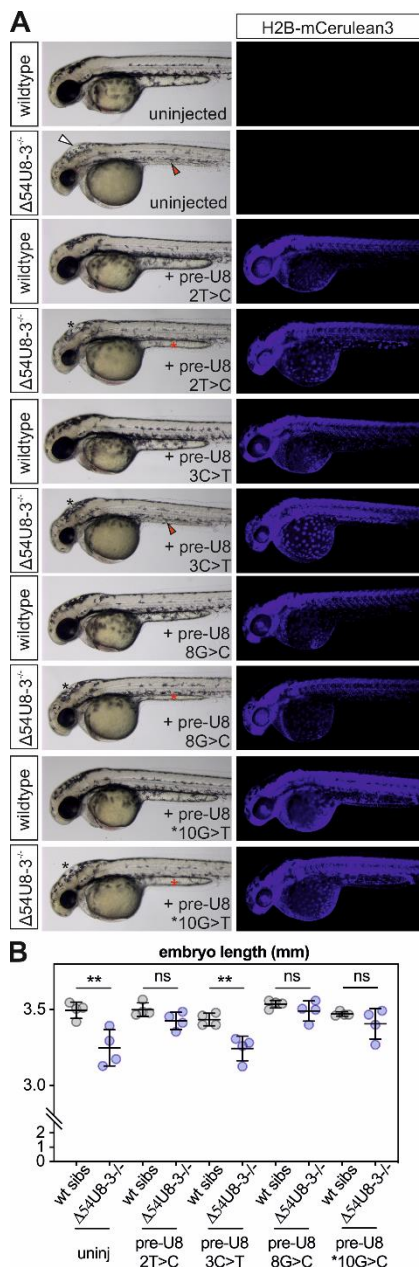


Figure S11. Functional testing of four LCC mutant U8 snoRNAs in zebrafish

A) Representative images of rescue experiments conducted with four putatively hypomorphic U8 mutations detected in LCC individuals. White arrowhead indicates hindbrain swelling and red arrowheads indicate abnormal yolk extension. Black and red asterisks indicate rescued hindbrain swelling and yolk extension respectively.

B) pre-U8^{3C>T} does not rescue the reduced embryo length of $\Delta U8-3$ mutants, whereas pre-U8^{2T>C}, pre-U8^{8G>C} and pre-U8^{*10G>T} restores $\Delta U8-3$ mutant embryo length to that of wildtype siblings. n=4 embryos per genotype. *Error bars* indicate S.D. from the mean.

C) alignment of human U8 and zebrafish U8 28S interaction region. Shared identity between zebrafish and human 28S-binding nucleotides is shown in pink.

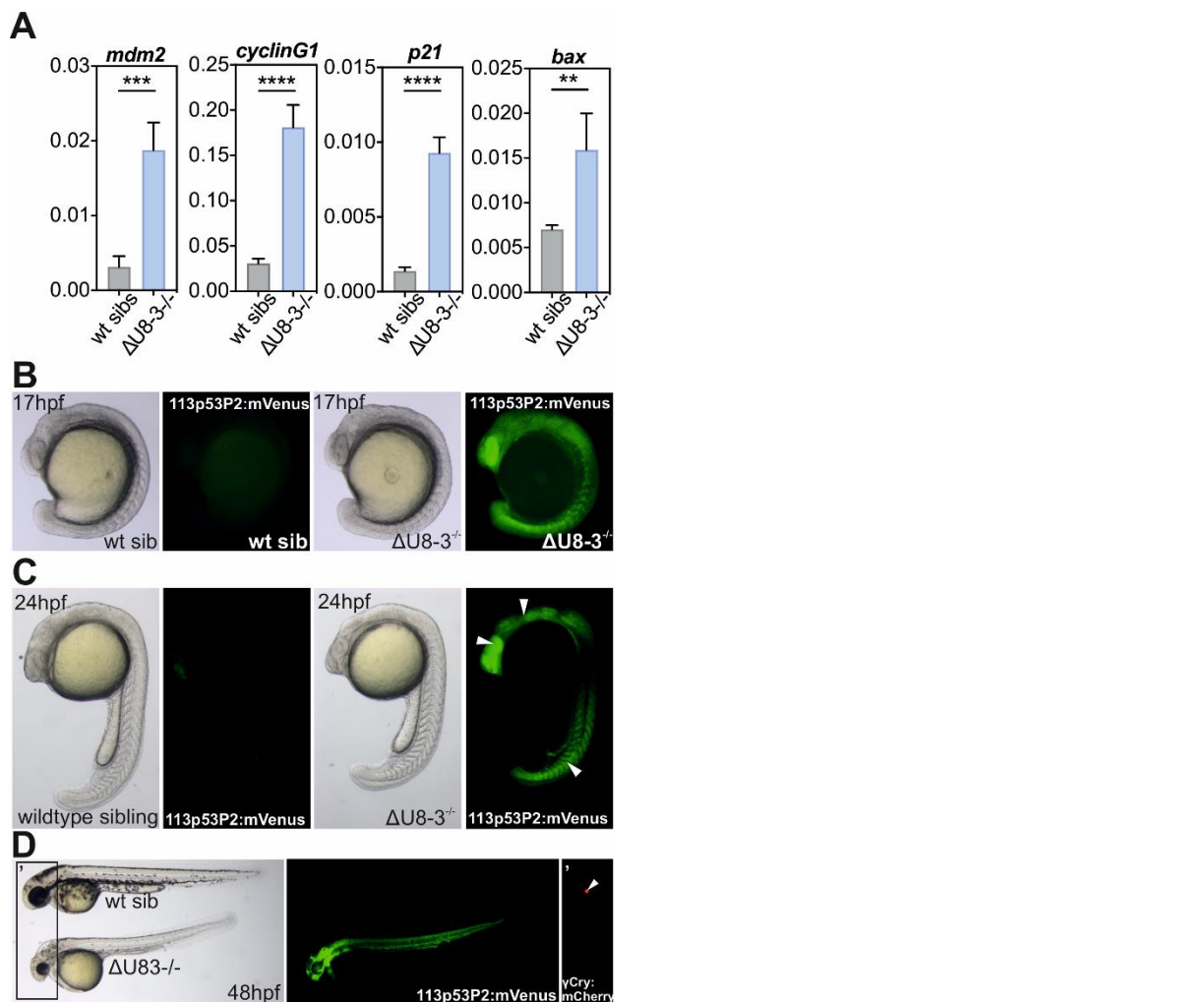


Figure S12. tp53 is trans-activated in response to loss of *U8-3* in zebrafish

A) quantitative RT-PCR demonstrates significant upregulation of the tp53 target genes *mdm2*, *cyclinG1*, *p21* and *bax* in $\Delta U8-3$ mutants when compared to wildtype siblings at 24hpf. Error bars indicate S.D. from the mean.

B) tp53 activity is observed throughout the $\Delta U8-3$ mutant at 17hpf, prior to the onset of observable gross morphological abnormalities, particularly in the eye.

C) tp53 activity is observed in numerous tissues that develop abnormally in $\Delta U8-3$ mutants, including the eye, hind-brain and somites (arrowheads) at 24hpf.

D) tp53 activity is observed throughout the $\Delta U8-3$ mutant at 48hpf. Integrated 113p53P2:mVenus transgene is reported by γ -crystallin:mCherry in the backbone of the plasmid which drives lens specific mCherry expression from approximately 36hpf. The developmental delay in $\Delta U8-3$ mutants delays expression of this reporter.

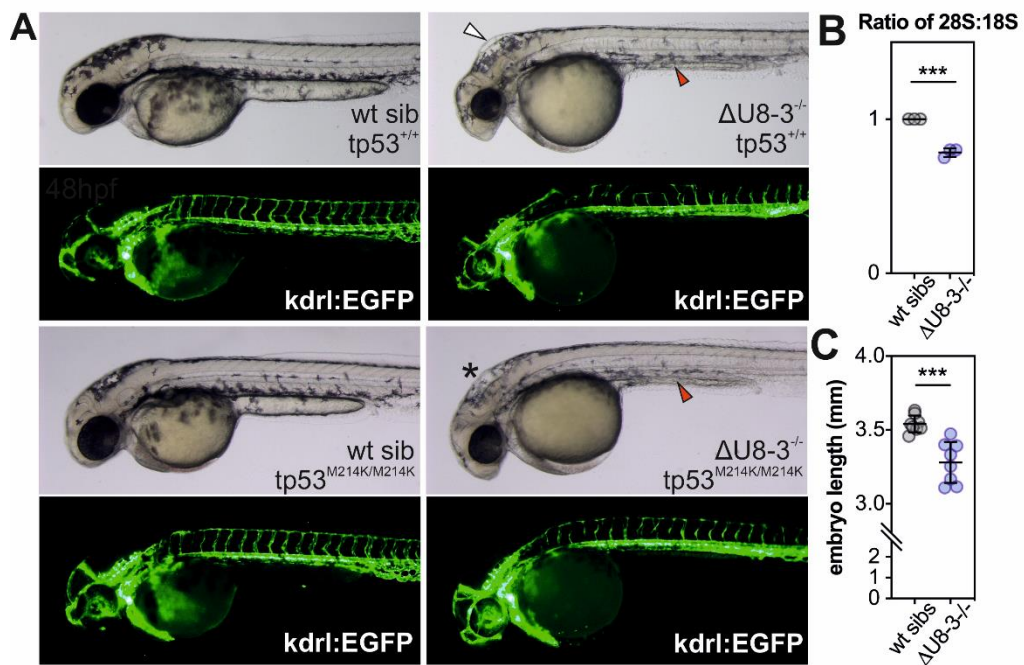


Figure S13. Inactivation of tp53 partially rescues the Δ U8-3 mutant phenotype although fails to rescue the embryo length or rRNA biogenesis defect

A) Representative images showing inactivation of tp53 signaling rescues the hindbrain swelling of Δ U8-3 mutants (white arrowhead compared to black asterisk) and the trunk vasculature, but not the yolk extension (red arrowhead) abnormality.

B) Tapestation assay demonstrates tp53 mutant Δ U8-3 mutant embryos display a preferential reduction in 28S biogenesis at 48hpf. n=3 biological replicates per genotype. Error bars indicate S.D. from the mean.

C) tp53 mutant Δ U83 mutant embryos are significantly shorter than tp53 mutant Δ U8-3 wildtype sibling embryos at 48hpf. n=8 biological replicates per genotype. Error bars indicate S.D. from the mean.

Table S1. LCC cohort published in Jenkinson 2016

Family	Number of affected individuals	Chromosomal position (Hg19)	Variants detected	Zygosity	gnomAD frequency
F172	1	g.8076761C>A	n.10*G>T	Het	0.002495
		g.8076851dup	n.56dup	Het	0.000008617
F278 #	1	g.8076832T>C	n.75A>G	Het	0.00001723
		g.8076899C>G	n.8G>C	Het	0.00001523
F281	1	g.8076826C>G	n.81G>C	Het	Novel
		g.8076904G>A	n.3C>T	Het	0.001482
F285	1	g.8076766G>C	n.*5C>G	Het	0.0006056
		g.8076850C>T	n.57G>A	Het	0.00002657
F309	1	g.8076776G>C	n.131C>G	Het	0.00001520
		g.8076904G>A	n.3C>T	Het	0.001482
F330	1	g.8076825T>C	n.82A>G	Het	0.00006832
		g.8076899C>T	n.8G>A	Het	0.002756
F331	2	g.8076761C>A	n.*10G>T	Het	0.002495
		g.8076835T>C	n.72A>G	Het	0.00006894
F334	1	g.8076825T>C	n.82A>G	Het	0.00006832
		g.8076761C>A	n.*10G>T	Het	0.002495
F337	1	g.8076905A>G	n.2T>C	Het	0.00002167
		g.8076849dup	n.58dup	Het	Novel
F343	1	g.8076766G>C	n.*5C>G	Het	0.0006056
		g.8076885_8076913dup	n.-7_22dup	Het	Novel
F344	1	g.8076794G>A	n.113C>T	Hom	0.00004177
		g.8076899C>G	n.8G>C	Hom	0.00001523
F362	2	g.8076766G>C	n.*5C>G	Het	0.0006056

		g.8076887G>A	n.20C>T	Het	0.00003021
F414	1	g.8076770G>A	n.*1C>T	Het	0.005054
		g.8076846T>C	n.61A>G	Het	0.00006073
F426	2	g.8076766G>C	n.*5C>G	Het	0.0006056
		g.8076826C>T	n.81G>A	Het	0.00004740
F433	1	g.8076766G>C	n.*5C>G	Het	0.0006056
		g.8076887G>A	n.20C>T	Het	0.00003021
F445	1	g.8076766G>C	n.*5C>G	Het	0.0006056
		g.8076780G>C	n.127C>G	Het	0.00004316
F446	1	g.8076766G>C	n.*5C>G	Hom	0.0006056
F454	2	g.8076766G>C	n.*5C>G	Het	0.0006056
		g.8076955_8076960del	n.-54_-49del	Het	Novel
F465	1	g.8076825T>C	n.82A>G	Het	0.00006832
		g.8076846_8076847insA	n.60_61insT	Het	0.000007591
F521	2	g.8076803C>T	n.104G>A	Het	0.0004176
		g.8076776G>C	n.131C>G	Het	0.00001520
F551	1	g.8076762G>A	n.*9C>T	Het	0.001923
		g.8076780G>C	n.127C>G	Het	0.00004316
F564	1	g.8076770G>A	n.*1C>T	Het	0.005054
		g.8076781G>A	n.126C>T	Het	0.0001178
F691	1	g.8076762G>A	n.*9C>T	Het	0.001923
		g.8076849T>C	n.58A>G	Het	0.00002277
F730	1	g.8076761C>A	n.*10G>T	Het	0.002495
		g.8076826C>T	n.81G>A	Het	0.00004740
F766	1	g.8076865C>T	n.42G>A	Het	0.001070
		g.8076904G>T	n.3C>A	Het	0.000004327
F780	2	g.8076770G>A	n.*1C>T	Het	0.005054
		g.8076776G>C	n.131C>G	Het	0.00001520

F819	2	g.8076762G>A g.8076770G>A g.8076696_8076977del§	n.*9C>T n.*1C>T	Het Het Het	0.001923 0.005054 Novel
F906	1	g.8076804C>T g.8076868C>G	n.103G>A (<i>de novo</i>) n.39G>C	Het Het	0.00001724 0.0001253
F1127	1	g.8076762G>A g.8076807A>C	n.*9C>T n.100T>G	Het Het	0.001923 Novel
F1172	1	g.8076762G>A g.8076776G>C	n.*9C>T n.131C>G	Het Het	0.001923 0.00001520
F1288	1	g.8076848A>C g.8076762G>A	n.59T>G n.*9C>T	Het Het	Novel 0.001923
F1424	1	g.8076777A>G g.8076912C>T	n.130T>C n.-6G>A	Het Het	0.000008628 0.0008539
F1445	1	g.8076904G>A g.8076826C>T	n.3C>T n.81G>A	Het Het	0.001482 0.00004740

#Also reported in McNeill N et al. Neurol Genet 14: e162 (2017)

Bolded mutations proposed to be hypomorphic – individuals highlighted in green lack mutations in any of the affected seven nucleotides located in the novel base-pairing region between the 5' end and 3' extension.

Nomenclature in gnomAD does not correspond to nomenclature in Alamut

Het = heterozygous; Hom = homozygous. gnomAD = Genome Aggregation Database

§ Deletion extends beyond these boundaries, but boundaries have not been fully defined. One sib carries g.8076762G>A

plus g.8076696_8076977del. The other sib carries g.8076770G>A plus g.8076696_8076977del. Mum carries g.8076762G>A plus g.8076770G>A.

Table S2. Oligonucleotides used in this study

PURPOSE	OLIGONUCLEOTIDE SEQUENCE 5' TO 3'
Sequence zebrafish U81 from genomic DNA	S ACGATACCACAATGCTGTAC AS GTAAGGATAACACAGAATACC
Sequence zebrafish U82 from genomic DNA	S CTCCACCAATAGTATCGCAG AS CTGTGGTGAAGTAACTTTC
Sequence zebrafish U83 from genomic DNA	See Genotype Δ54U8-3 allele
Sequence zebrafish U84 from genomic DNA	S CCAATAGGATCACAGGAGAC AS GCATAGTAAGCTATA GTGCTC
Sequence zebrafish U85 from genomic DNA	S GGAGCATTAGCATGCTAAC AS TTTCTAGCACACCCCTGCTG
Quantitative RT-PCR to U8-1	S GGTTTATCCTTACCTGTTGTC AS CAGACAGGATTCTAAAGGTC
Quantitative RT-PCR to U8-2	S ACATCAGTGAGGTTTGTG AS CACATAGGATCCAGAGTTGTG
Quantitative RT-PCR to U8-3	S GAGGTACATCCTTACCTGTTAC AS GATT CGTAAAGGGGTTGCAG
Quantitative RT-PCR to U8-4	S GGTTTATCCTTACCTGTTGTC AS TAAAGAGGTTGCAAGTCATG
Quantitative RT-PCR to U8-5	S GCATCAGTGAGGTTATCCTTG AS CAAGCCCTATATGAACACAGAG
DNA template for production of guide RNA to cleave 5' of U8-3	S TAATACGACTCACTATAAGGCCTCGTTAAAAGCATGTGGTTTAGAGC AS AAAAGCACCAGACTCGGTGCCACTTTCAAG
DNA template for production of guide RNA to cleave 3' of U8-3	S TAATACGACTCACTATAAGGCCTCGGTGCCACTTTCAAG AS AAAAGCACCAGACTCGGTGCCACTTTCAAG
DNA template for production of guide RNA specific to U8-3	S TAATACGACTCACTATAAGATCTGAA CCTTATTGCTAGTTTAGAGC AS AAAAGCACCAGACTCGGTGCCACTTTCAAG
Genotype ΔU8-3 allele	S1 ACCCTTGACAGAGGAGTTG S2 TCCAATCCAACCAATGAGAC AS CATGCAGAAAATGTCCTACTATC S TAAACGATCGTCTCGTCCAC AS GGAATGGAGTCACAGACTTAC
Genotype Δ54U8-3 allele	S TAATACGACTCACTATAAGGGACATCAGTGAGGTACATCC AS GTCAGACAGGATTCTGAAAG
DNA template for production of zebrafish U8-3 snoRNA	S TAATACGACTCACTATAAGGGACATCAGTGAGGTACATCC AS GGT TATTAAAATGTGTCAAGACAGGATT
DNA template for production of zebrafish pre-U8-3 snoRNA	S TAATACGACTCACTATAAGGGATCGTCAGGTGGGATAATCC AS AATCAGACAGGAGCAATCAGGGTGTGCAAG
DNA template for production of human U8 snoRNA	S TAATACGACTCACTATAAGGGATCGTCAGGTGGGATAATCC AS ACAAATGTAAGTGTCTCG
DNA template for production of human pre-U8 snoRNA	S TAATACGACTCACTATAAGGGATCGTCAGGTGGGATAATCC AS ACAAATGTAAGTGTCTCG
DNA template for production of human pre-U8 snoRNA 57G>A	S STAATACGACTCACTATAAGGGATCGTCAGGTGGGATAATCCTTACCTGTTCCCTCCG GAGGGCAGATTAGAACATAATGATTGGAGATGCATG AS ACAAATGTAAGTGTCTCG
DNA template for production of human pre-U8 snoRNA 58A>G	S STAATACGACTCACTATAAGGGATCGTCAGGTGGGATAATCCTTACCTGTTCCCTCCG GAGGGCAGATTAGAACATGTTGAGATGCATG AS ACAAATGTAAGTGTCTCG
DNA template for production of human pre-U8 snoRNA 61A>G	S STAATACGACTCACTATAAGGGATCGTCAGGTGGGATAATCCTTACCTGTTCCCTCCG GAGGGCAGATTAGAACATGTTGAGATGCATGAAAC AS ACAAATGTAAGTGTCTCG
DNA template for production of human pre-U8 snoRNA *1C>T	S TAATACGACTCACTATAAGGGATCGTCAGGTGGGATAATCC AS ACAAATGTAAGTGTCTCG
DNA template for production of human pre-U8 snoRNA *5C>G	S TAATACGACTCACTATAAGGGATCGTCAGGTGGGATAATCC AS ACAAATGTAAGTGTCTCG
DNA template for production of human pre-U8 snoRNA *9C>T	S TAATACGACTCACTATAAGGGATCGTCAGGTGGGATAATCC AS ACAAATGTAAGTGTCTCG
DNA template for production of human pre-U8 snoRNA 2T>C	S TAATACGACTCACTATAAGGGACCGTCAGGTGGGATAATCCTTACC AS ACAAATGTAAGTGTCTCG
DNA template for production of human pre-U8 snoRNA 3C>T	S TAATACGACTCACTATAAGGGATTGTCAGGTGGGATAATCC AS ACAAATGTAAGTGTCTCG
DNA template for production of human pre-U8 snoRNA 8G>C	S TAATACGACTCACTATAAGGGATCGTCAGGTGGGATAATCCTTACC AS ACAAATGTAAGTGTCTCG
DNA template for production of human pre-U8 snoRNA *10G>T	S TAATACGACTCACTATAAGGGATCGTCAGGTGGGATAATCC AS ACAAATGTAAGTGTCTCG
Amplification of 113p53 promoter	S GACAGACTCGAGTAGCTCGTGGCTGACATC AS GACAGAACTAGTAGCTGCA GTTTGTGCTGTG
Quantitative RT-PCR to zebrafish Δ113p53	S ATATCCTGGCGAACATTGG AS ACGTCCACCAACCATTGAAC
Quantitative RT-PCR to zebrafish mdm2	S TGACAACGAGAACTGGTAAGA AS AAACATAACCTCCTTGTG
Quantitative RT-PCR to zebrafish p21	S AGCTGCATT CGTCTCGTAGC AS CGGTTGAAATAAAACGGAATA

Quantitative RT-PCR to zebrafish cyclinG1	S GTGC GGAGAC GCTT CTT AS AAGACAGATGCTTGGCTGA
Quantitative RT-PCR to zebrafish bax	S GGAGGC GATA CGGG CAGTG AS TCGG CTGA AGATTAGAG TTGTTT
Quantitative RT-PCR to zebrafish elf1a	S CTGG AGGC CAGC TCAA AC AS ATCA AGAA AGAG TAGT ACCG CTAG CATT AC
Genotyping of the M214K substitution in p53 mutant zebrafish. The p53 locus is amplified with S1-AS1 for 35 cycles. 1ul of the PCR product is used as a DNA template for amplification with S2-AS2. Sequencing is performed with M13 Probe sequence for human 3'-ETS - LD2612	S1 CCATGTAGTGAAGTATAGTTGC AS1 GTCGGGTCTTCAGTTTATGC S2 TGAAAACGACGCCAGTGAATTATATCAA AS2 AGGAAACAGCTATGACCATCCAATGGCATG M13 CAGGAAACAGCTATGAC
	GAGGAGGC GGG AACCGA AGAAC GCGG